

**ОПТИЧЕСКИЕ ХАРАКТЕРИСТИКИ АЛЮМИНИЯ С
ГОРЯЧИМИ ЭЛЕКТРОНАМИ И КИНЕТИКА
ПЛАВЛЕНИЯ ПОД ДЕЙСТВИЕМ
УЛЬТРАКОРОТКОГО ЛАЗЕРНОГО ИМПУЛЬСА**

**С.И. Анисимов(1), Н.А. Иногамов(1), Ю.В. Петров(1), В.А.
Хохлов(1), М.Б. Агранат(2), С.И. Ашитков(2), В.В.
Жаховский(2,3),
К. Nishihara(3)**

***(1) Landau Institute for Theoretical Physics,
RAS***

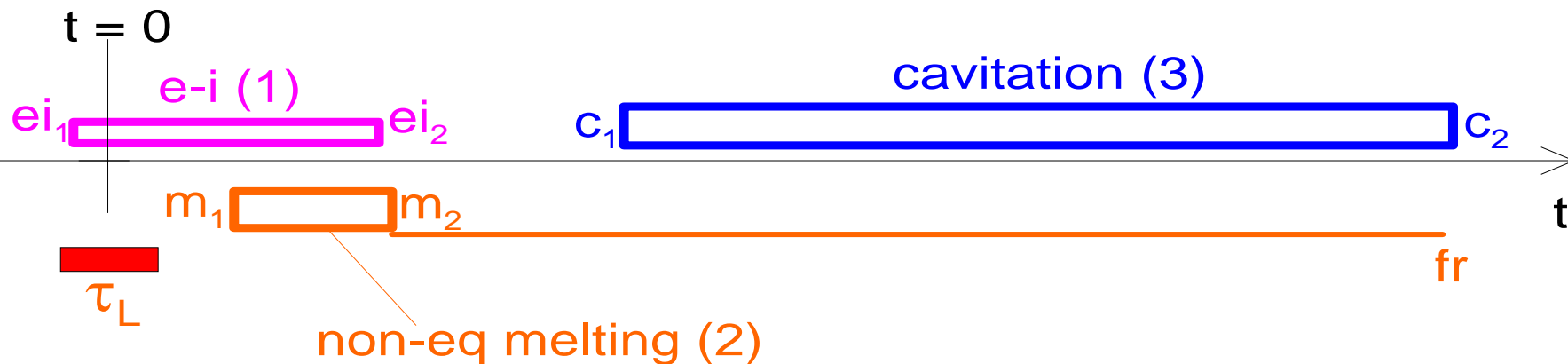
(2) Institute for High Temperatures, RAS

***(3) Institute for Laser Engineering, Osaka
University***

Chain of kinetics (1):(2):(3) initiated by pump fsLP

Pump fsLP \rightarrow (fsLP=femtosecond Laser Pulse, typ. 10-100 fs)

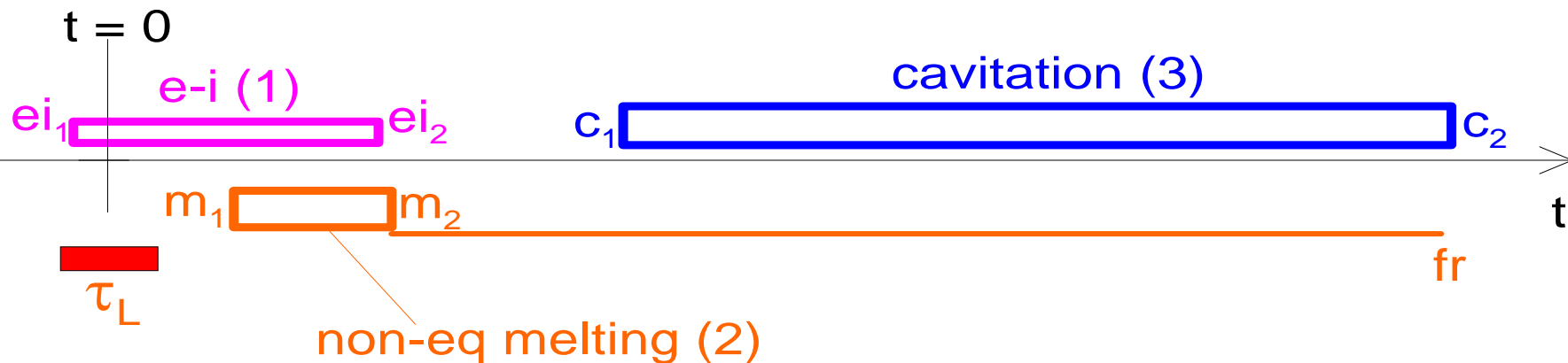
- **e-i relaxation** (e^- absorb $F_{abs} \rightarrow T_e$ is higher than $T_i \rightarrow e^-$ heat i =ions)
- Anisimov, Kapeliovich, Perel'man, JETP (1974).
- e^- overheating begins approximately together with fsLP
- F = fluence : J/cm² : fsLP energy surface density, abs = absorbed



Chain of kinetics (1):(2):(3) initiated by pump fsLP

Pump fsLP \rightarrow (fsLP=femtosecond Laser Pulse, typ. 10-100 fs)

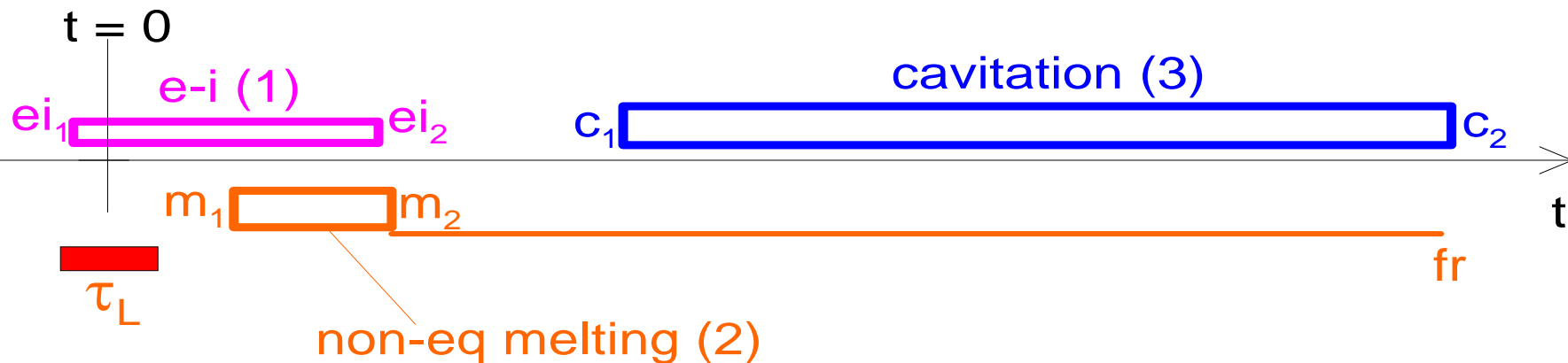
- **e-i relaxation** (e^- absorb $F_{abs} \rightarrow T_e$ is higher than $T_i \rightarrow e^-$ heat i =ions)
- **Non-equilibrium melting** with overheated crystal
- Equilibrium melting with well defined **melting front**

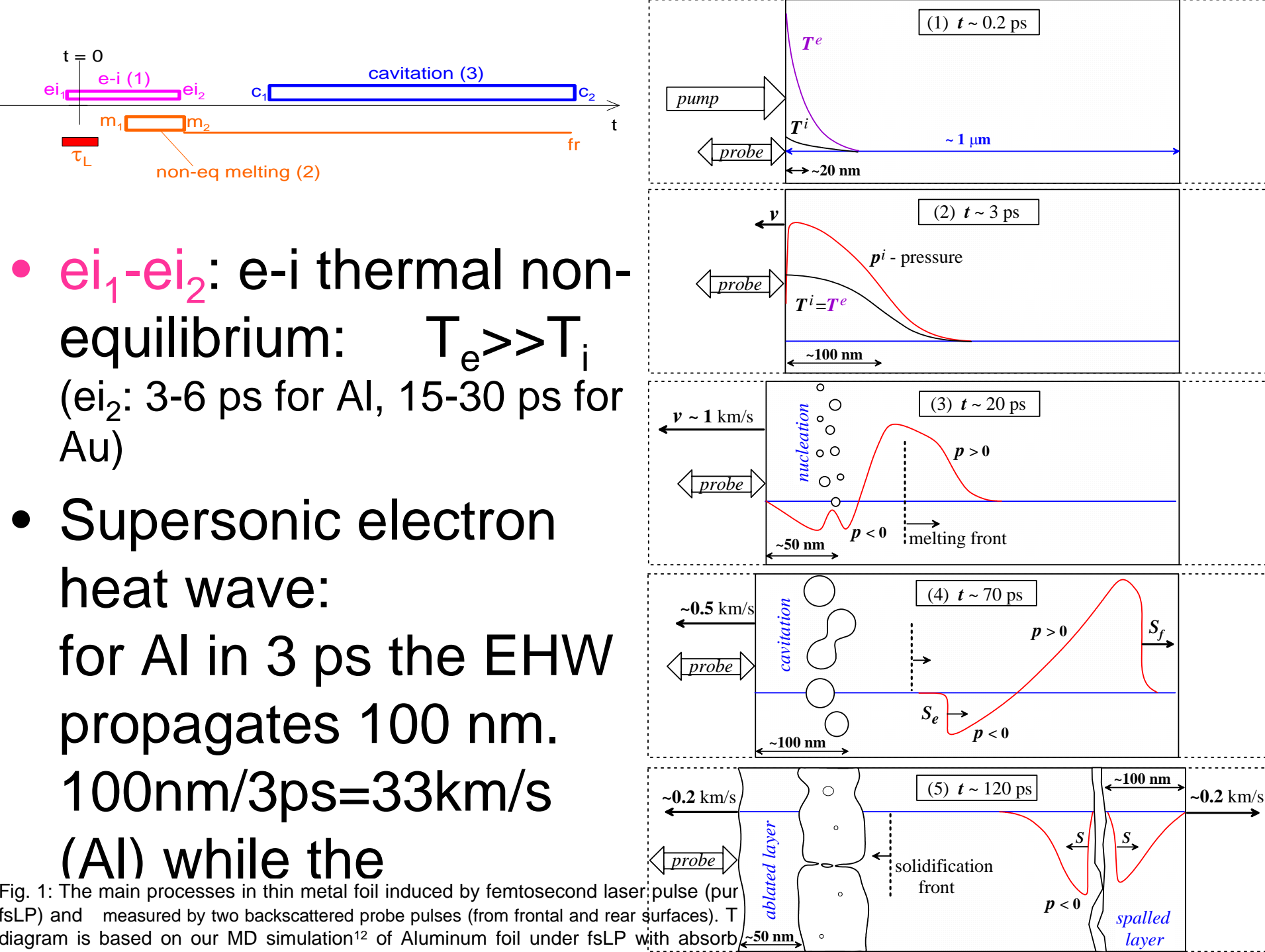


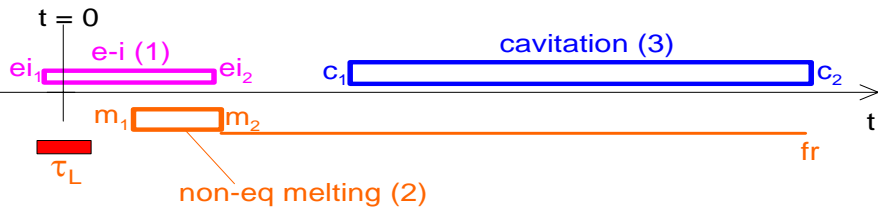
Chain of kinetics (1):(2):(3) initiated by pump fsLP

Pump fsLP \rightarrow (fsLP=femtosecond Laser Pulse, typ. 10-100 fs)

- **e-i relaxation** (e^- absorb $F_{abs} \rightarrow T_e$ is higher than $T_i \rightarrow e^-$ heat i =ions)
- **Non-equilibrium melting** with overheated crystal
- Equilibrium melting with well defined **melting front**
- **Cavitation** in metastable stretched liquid







- $ei_1 - ei_2$

- The supersonic EHW:

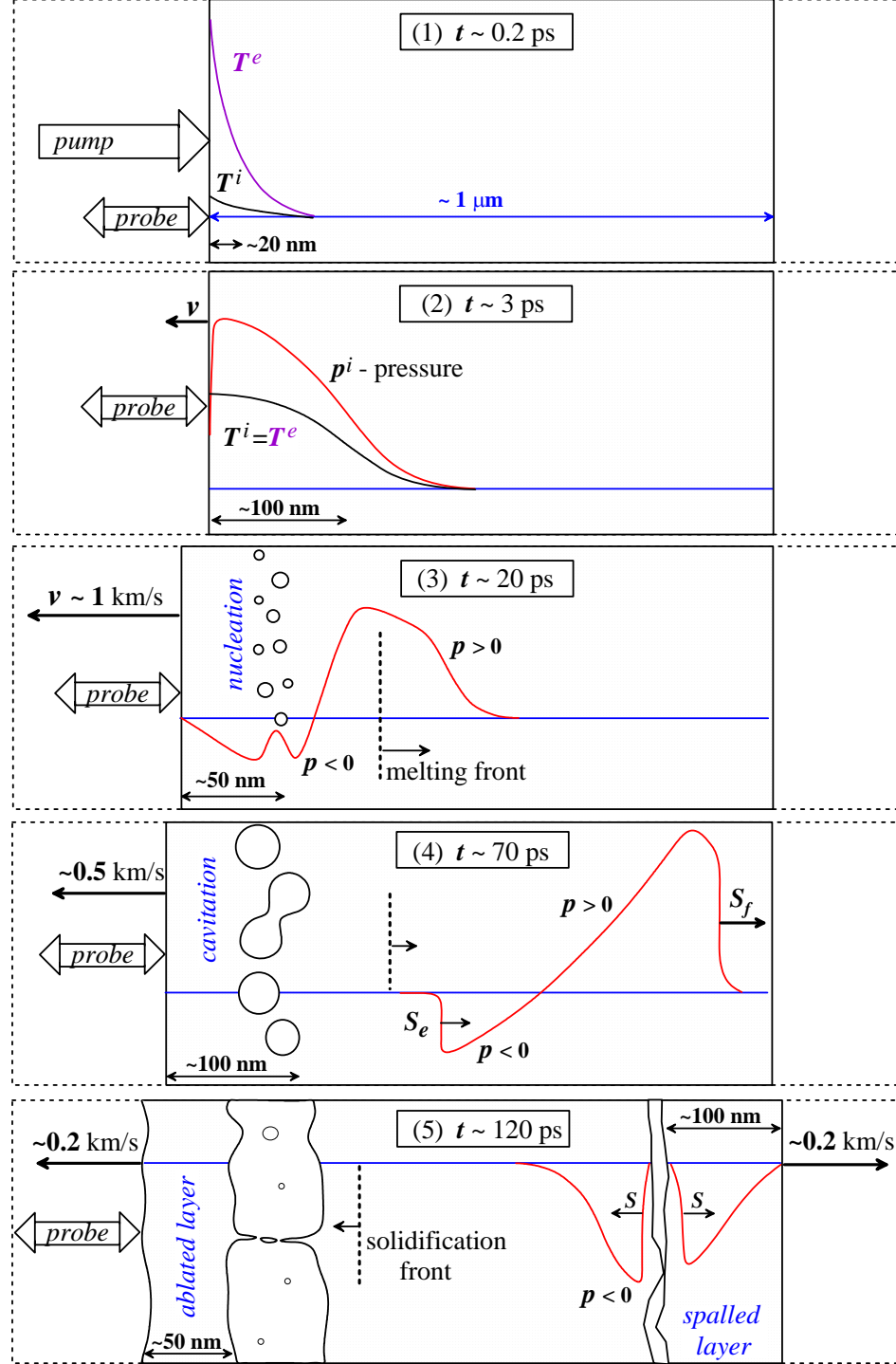
- $x = \sqrt{\chi t}$, $\chi = \frac{1}{3} v l$

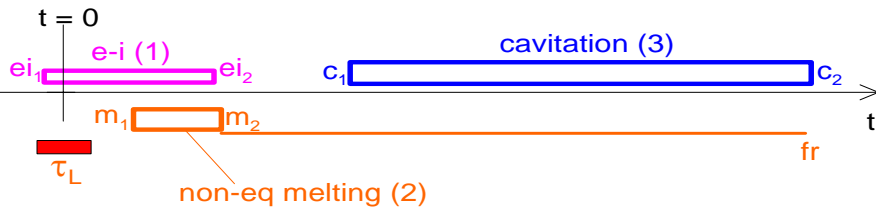
- $\tau = \frac{l}{v} \sim \text{few fs}$, $\sim \text{nm}$

- $v = 2000 \text{ km/s}$, $c_s = 5.5$

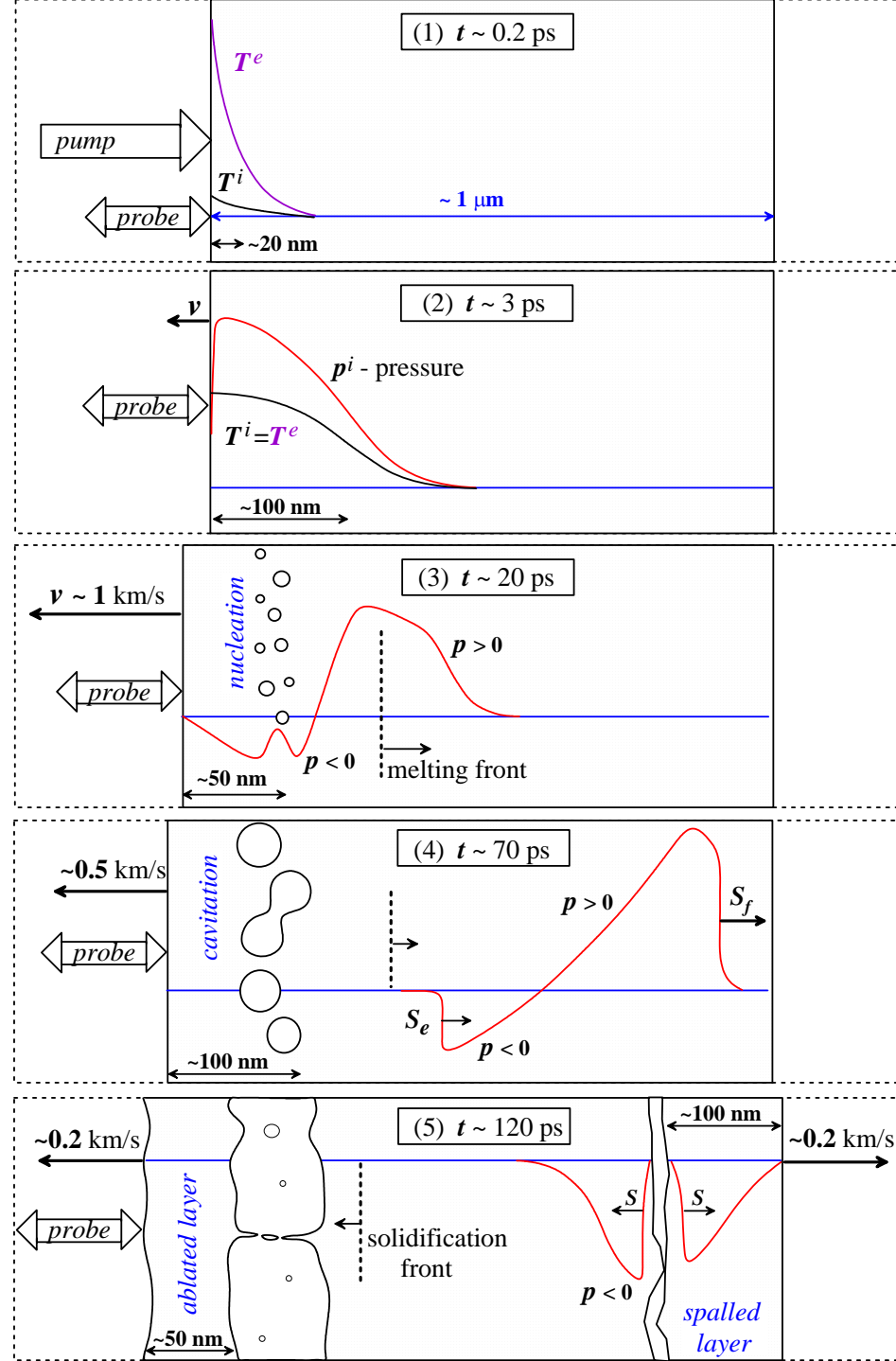
- $\frac{\text{km/s}}{c_s} = 400$, $v_T = \frac{dx}{dt}$

- $\frac{v_T}{c_s} \sim 100 \sqrt{\frac{\tau}{t}}$





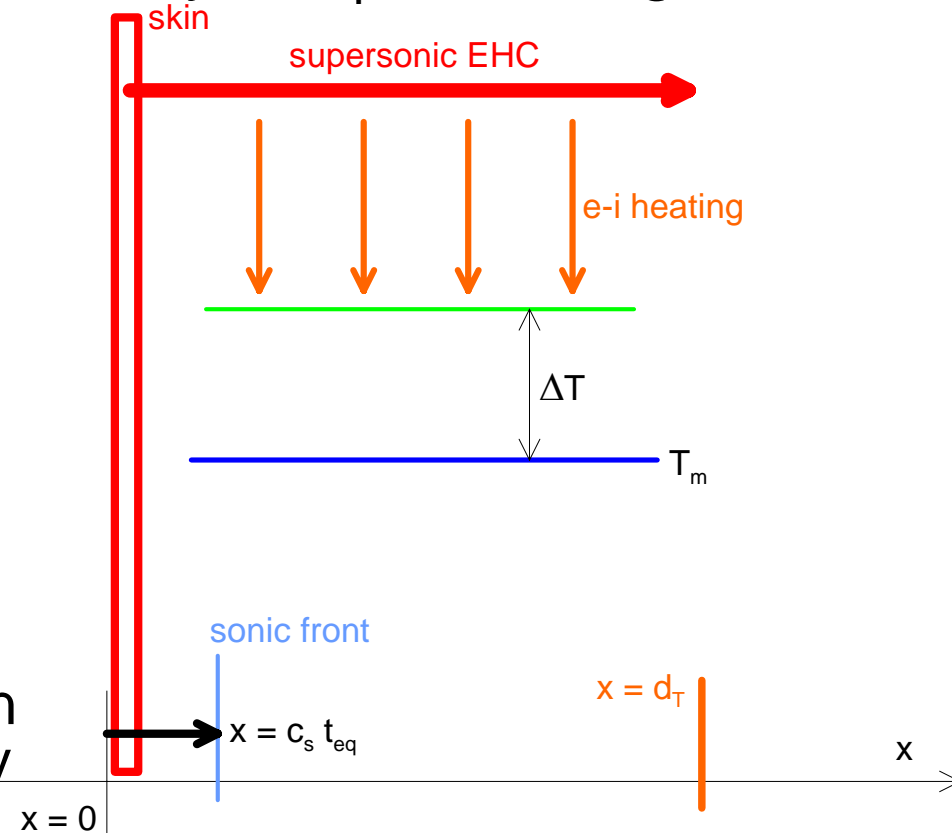
- **ei1-ei2**: e-i thermal non-equilibrium: $T_e \gg T_i$ (ei2: 3-6 ps for Al, 15-30 ps for Au)
- **m₁**: The **beginning** of non-eq melting depends on value of F_{abs} (**m₁**: 0.3-1 ps/Al, 1-5 ps/Au)
- **m₂**: The **end** of the non-eq melting



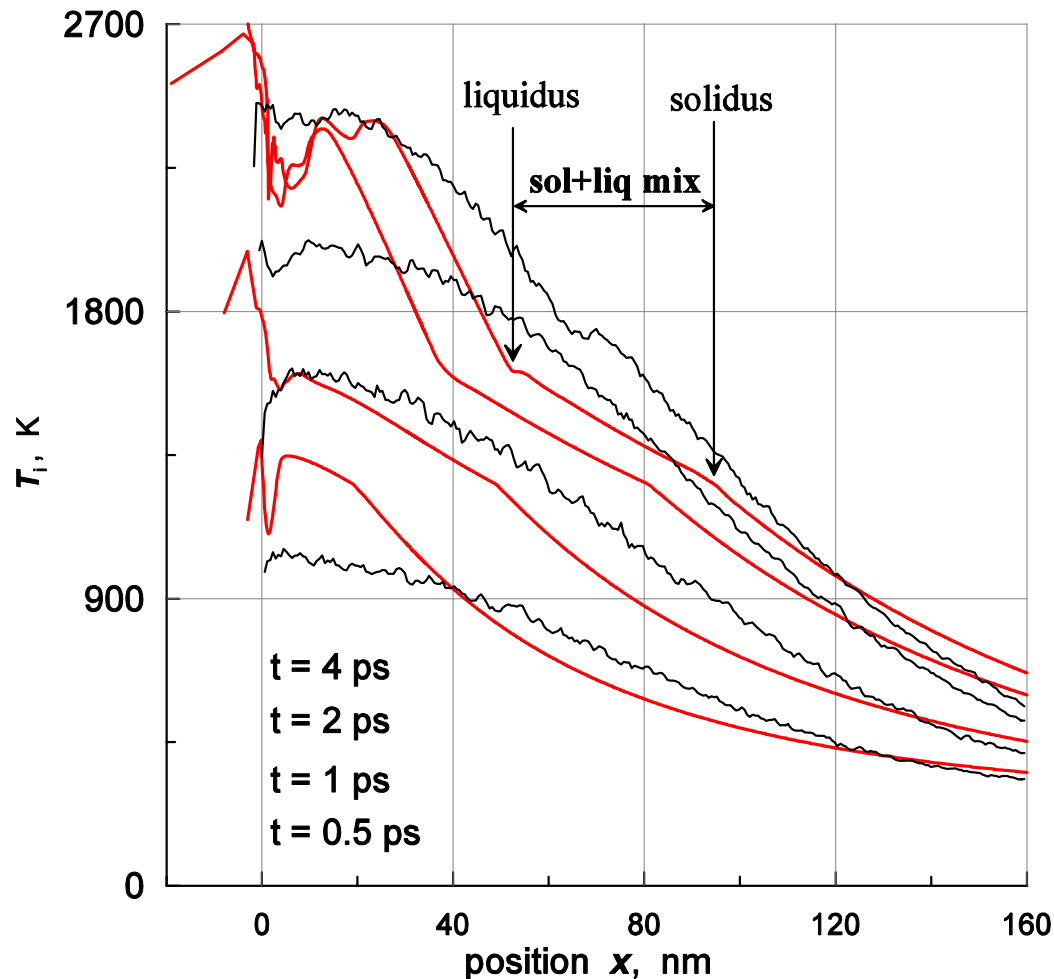
Initially supersonic electron Heat Wave and Creation of thick heated Layer

- The pump fsLP at considered fluencies at early stages strongly overheats electrons above ions during the time interval t_{eq} . Very fast (Mach ~ 10 , $c_s t_{eq} \ll d_T$) electron heat conduction wave (EHC) propagates deep into bulk creating ~ 100 nm thick heated layer d_T in Al target.

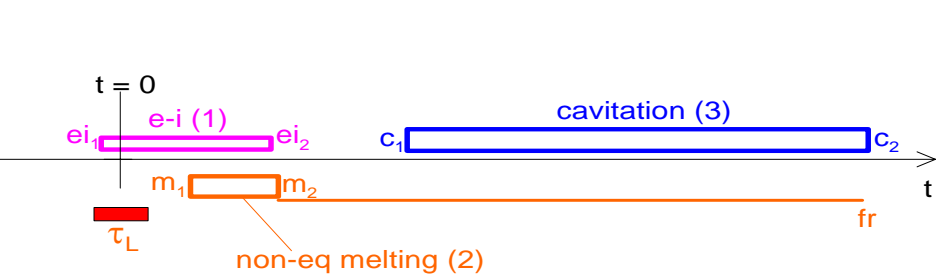
- The electron cooling by the electron-ion energy exchange heats ions – their temperature T_i gradually rises, and at $F \sim F_{abl}$ and higher the T_i significantly overcomes melting temperature $T_m(p)$ – an overheated solid appears and the non-equilibrium melting starts. The significant excess over T_m is possible because the heating is fast and there is enough thermal energy in the electrons – F_{abl} is significantly higher than F_{melt} – melting threshold



Heating the ion subsystem by energy transfer from hot electron subsystem



- This Figure illustrates how Ti increases in time
- Fabs = 65 mJ/cm²



- **C1:** (nucleation in melt is called **cavitation**)
- $P > 0$ versus $P = 0 \rightarrow v \rightarrow \rightarrow$ a density drop \rightarrow stretching $\rightarrow P < 0$
- $|P < 0| = P_{\text{neg}} (F_{\text{abs}})$, $P_{\text{neg}} (F_{\text{abs}}) \text{ propto } F_{\text{abs}}$
- If $P_{\text{neg}} > P_{\text{strength}}$ of material \rightarrow **nucleation**

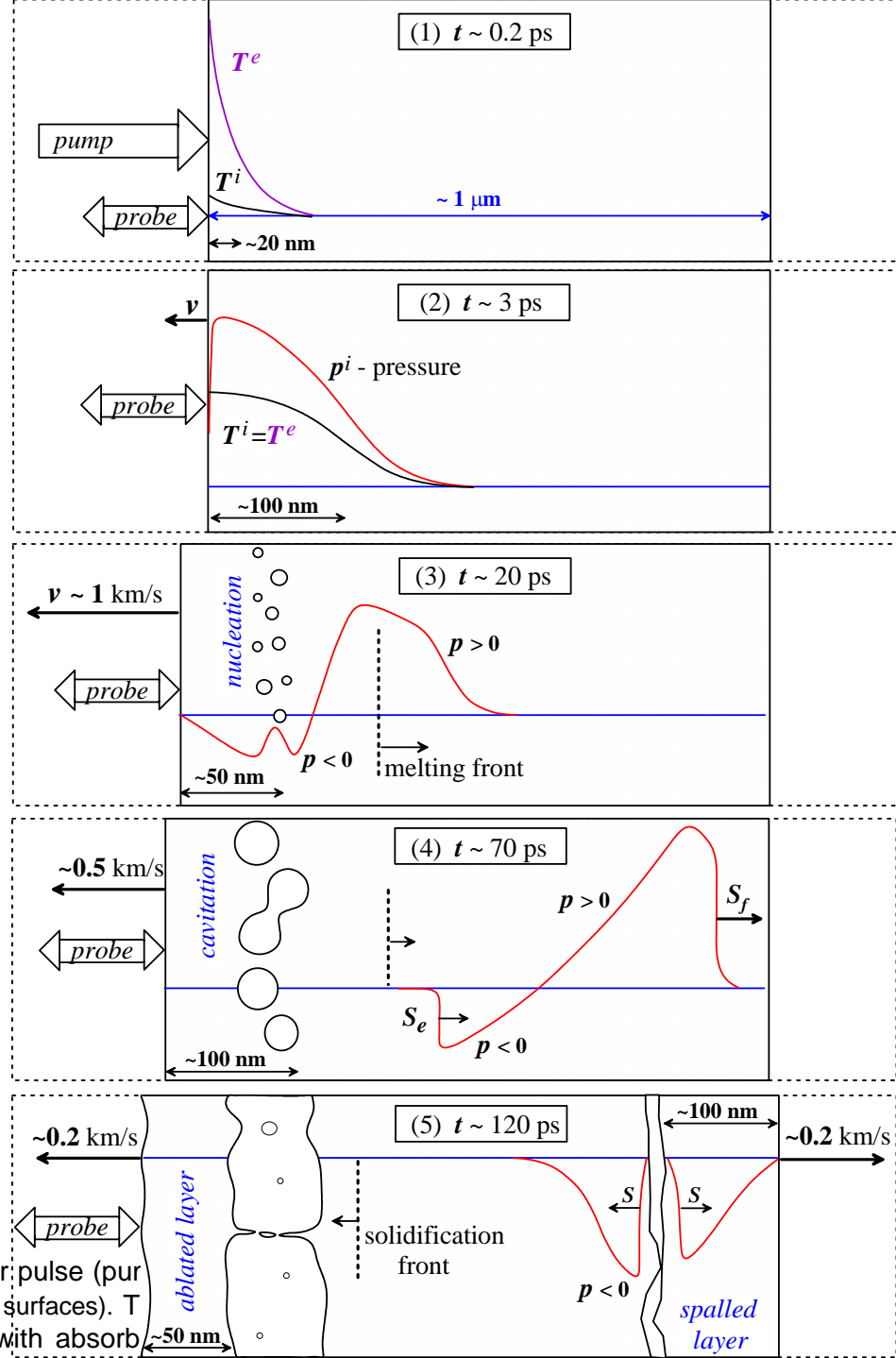
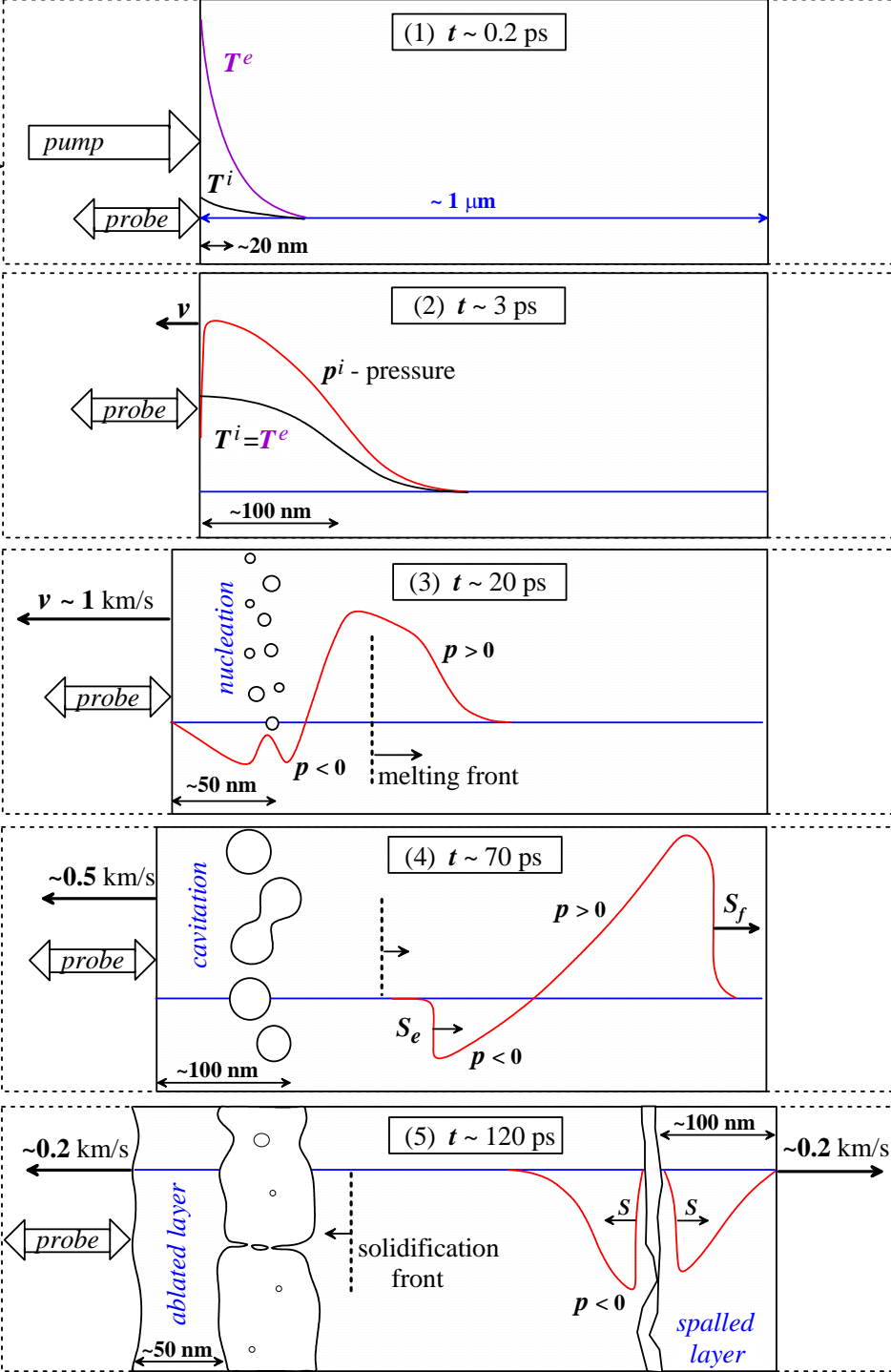
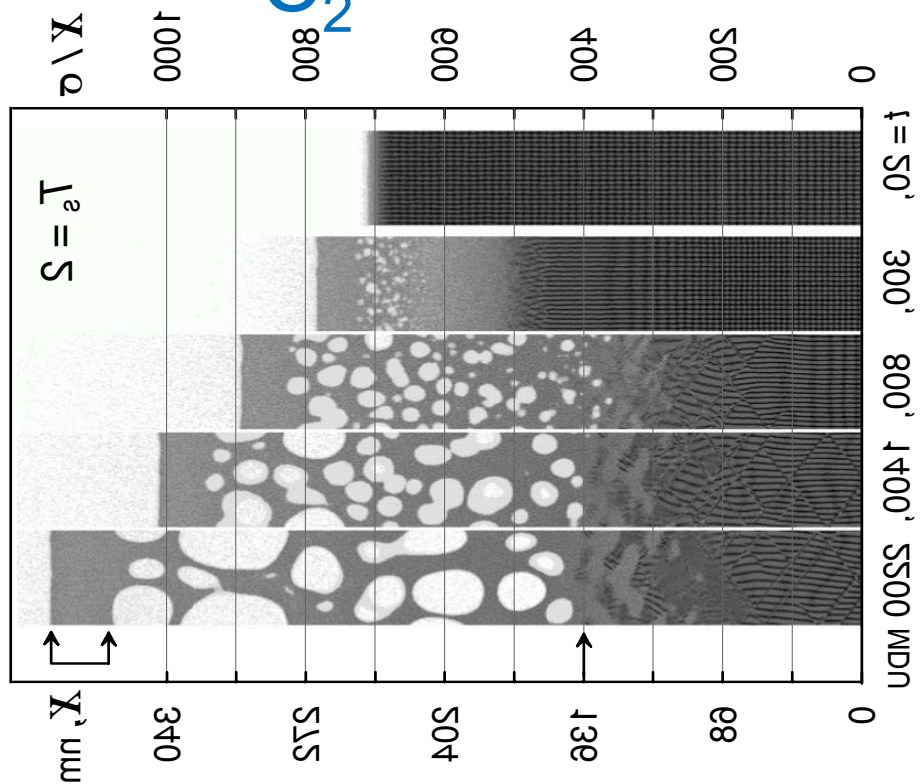
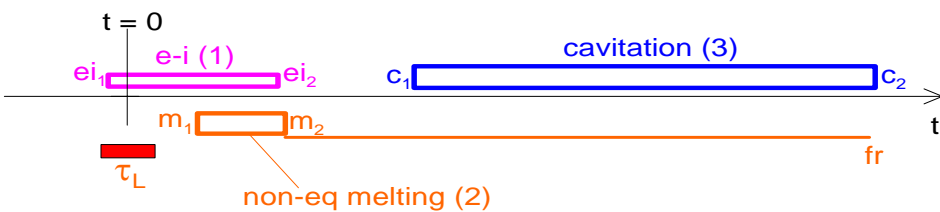


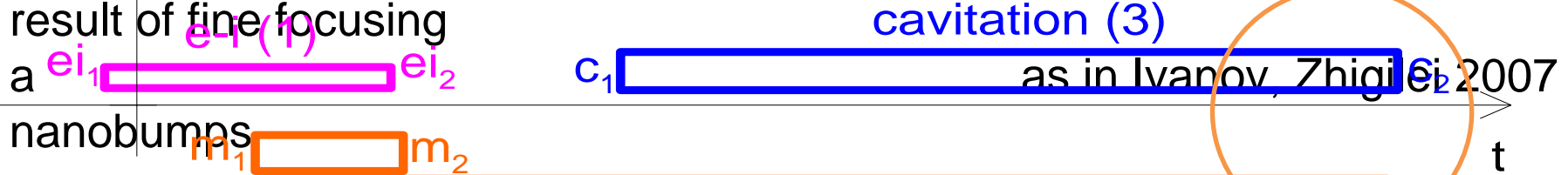
Fig. 1: The main processes in thin metal foil induced by femtosecond laser pulse (pump fsLP) and measured by two backscattered probe pulses (from frontal and rear surfaces). T diagram is based on our MD simulation¹² of Aluminum foil under fsLP with absorp

- C_1
- From C_1 to C_2



C₂ Nanorelief: transient and frozen

- Early stages: **2T**, **non-equilibrium melting**
- Intermediate and late stages: **equilibrium melting/solidification** and **cavitation**
- New mechanism of nanorelief growth. Surface perturbations grow at an ideal crystal face = this is not amplification of initial perturbation. This is not interaction of laser EM wave with reflected surface EM wave. Scale of relief is defined by a heat penetration depth (not EM wavelength). Also this is not result of fine focusing

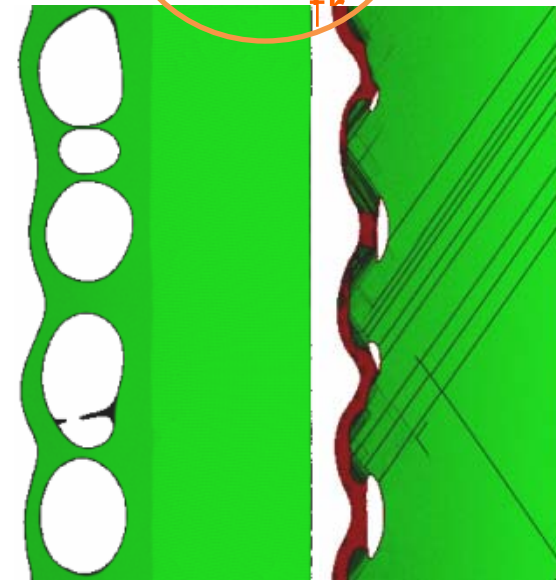


nanobumps

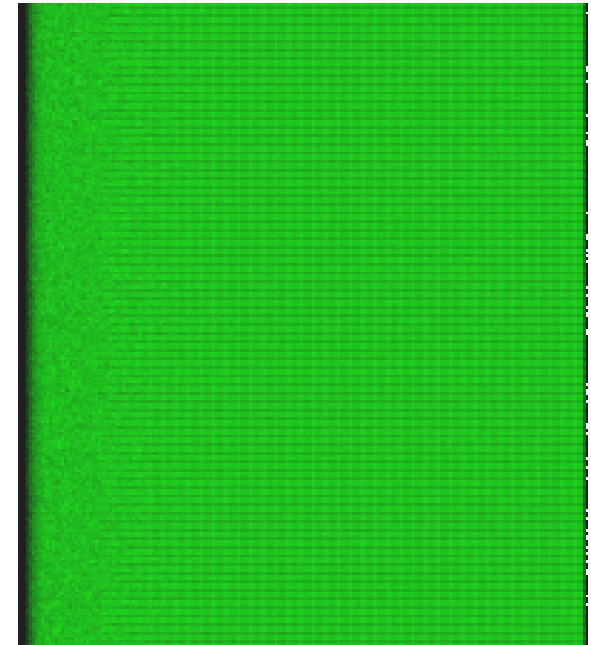
τ_L

non-eq melting (2)

- Dependence on parameters: run-away before it is frozen or it is frozen before run-away (mention current position of melting front)
- Rephasing during melting: at the transient phase the surface bumps are above the bubbles, while during cooling and re-crystallization the bubbles are compressed - therefore bumps are above frozen jets
- Bubbles remains frozen under surface



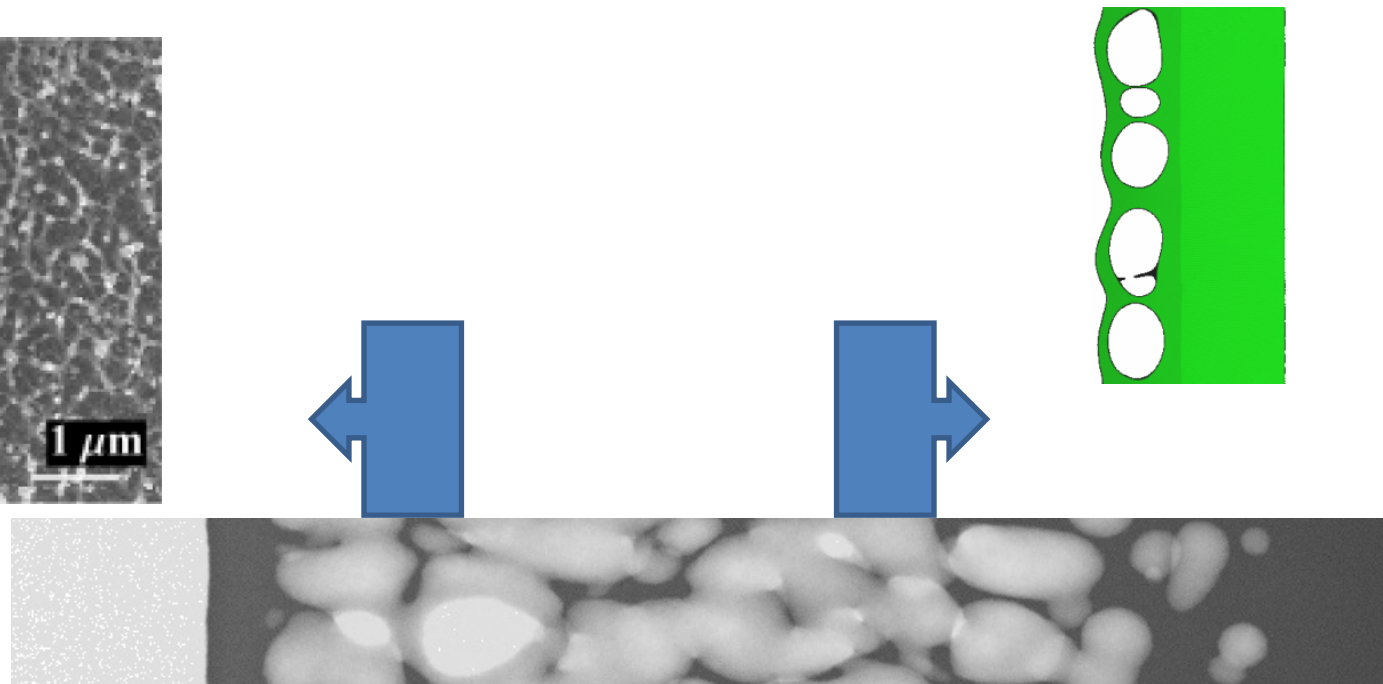
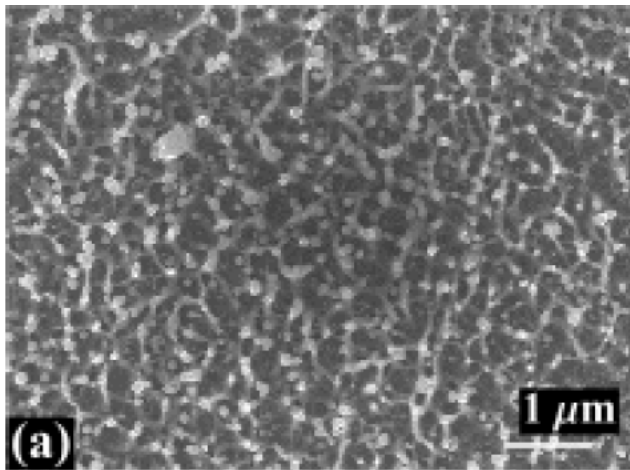
MD simulation of laser ablation of Aluminum crystal film



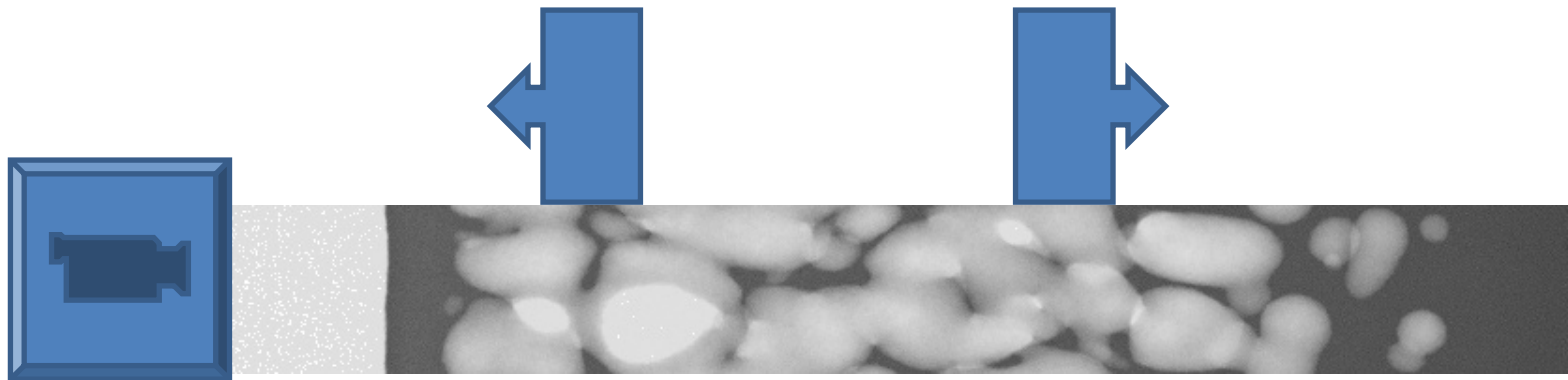
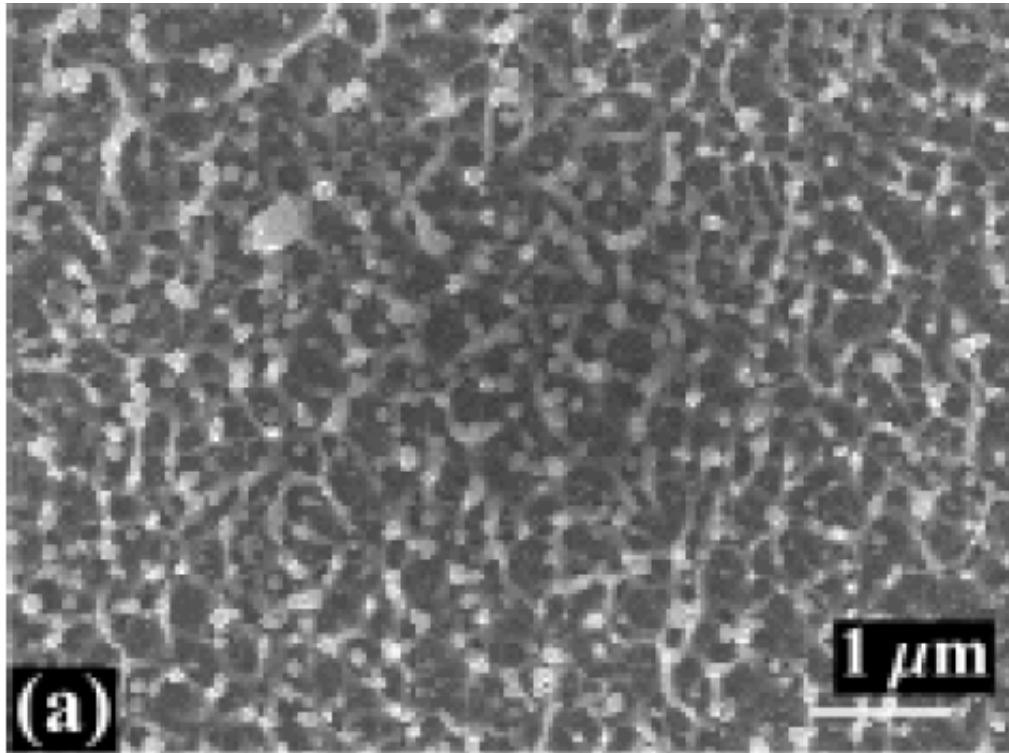
The wide Al target with cross section $L_y \times L_z = 122 \times 14 \text{ nm}^2$ heated up to the $T_0(0) = 5 \text{ kK}$ at the small heated depth $d_T = 18.6 \text{ nm}$. The total simulation time is 153.5 ps.

Run-away of a cavitation layer, inflation of foam, and cooling/solidification of the bottom layer of cavitation foam

- Two-phase region may be simple or reach and thick
- In the last case it breaks-up in the middle forming 1+2+3 parts:
- Part 1 returns to the running away layer
- Part 2 converts into droplet-vapor ejecta
- Part 3 keeps its ties with the bottom of a crater + moves very slowly + may be solidified with frozen bubbles or with frozen jets (compare with Vorobyev, Guo 2007)



Run-away of a cavitation layer, inflation of foam, and cooling/solidification of the bottom layer of cavitation foam



Model: 2Tgd + Helmholtz / EOS

$$\rho^0 \frac{\partial u}{\partial t} = - \frac{\partial p}{\partial x^0}$$

$$\rho^0 \frac{\partial (E_e / \rho)}{\partial t} = \frac{\partial}{\partial x^0} \left(\frac{\rho \kappa}{\rho^0} \frac{\partial T_e}{\partial x^0} \right) - p_e \frac{\partial u}{\partial x^0} - \frac{\rho^0}{\rho} \alpha (T_e - T_i) + \frac{\rho^0}{\rho} Q$$

$$\rho^0 \frac{\partial (E_i / \rho)}{\partial t} = p_i \frac{\partial u}{\partial x^0} + \frac{\rho^0}{\rho} \alpha (T_e - T_i)$$

$$F_{xx} + \varepsilon k^2 F = 0$$

- $P = P_i + P_e$; $P_i(\rho, T_i)$, $E_i(\rho, T_i)$ are taken from Bushman, Lomonosov, Fortov EOS (1992), while for $P_e(\rho, T_e)$, $E_e(\rho, T_e)$ free electron Fermi model is used

21 gd+Helmholtz /heat conduction & collisions

- Heat conduction coefficient is

$$\kappa = \frac{1}{3} \frac{v^2 C_e}{v}, \quad v^2 = \frac{2E_F + 3T_e}{m_e}, \quad v = (v_{ei} + v_{ee}) \left(\frac{\rho^0}{\rho} \right)^{1.3}$$

- Index “1.3” is taken from quantum MD of Desjarlais, 2002.
- Collision frequencies for kappa in solid and liquid phases are

$$v_{ei}^{sol} = 4.2 \cdot 10^{14} (T_i / T_3), T_3 = 933K$$

$$v_{ei}^{liq} = 1.1 \cdot 10^{14} T_i / (A + BT_i + C / T_i)$$

$$v_{ee}^{\kappa} = b_{\kappa} (E_F / \hbar) (T_e / T_F)^2$$

- The expression A+B T+C/T approximates data from quantum MD simulation of Al (Recoules, Crocombette, 2005).
- We use different values for coefficient “b” in nu_{ee} for heat conduction (superscript “kappa”) and for epsilon (superscript “epsilon”)

2Tgd+Helmholtz /Optics

- Computed $\rho(x,t)$, $f(x,t)$, $T_e(x,t)$, $T_i(x,t)$ instant profiles have been used for calculation of dielectric function $\epsilon(x,t)$. Here f is a volume fraction of liquid phase in mixture zone
- Profile $\epsilon(x,t)$ is necessary to solve Helmholtz equation for amplitude F of probe fsLP propagating normally to the target surface with wavevector k

$$F_{xx} + \epsilon k^2 F = 0$$

- Helmholtz eqn. \rightarrow reflectivity $R(t)$, phase $\Psi(t)$
- Dielectric function is calculated as a sum of the Drude and band-band components

$$\epsilon = 1 - \frac{\omega_{pl}^2}{\omega^2 + \nu^2} \left(1 - i \frac{\nu}{\omega} \right) + \Delta_{bb}$$

- Δ_{bb} (Ashcroft, Sturm ;1971) for solid Al

2Tgd+Helmholtz /Optics of mixtures

- There is a near surface layer of solid + liquid mixture at early stages of Al melting. Skin layer depth of the target gradually changes from solid to liquid state composition passing the mixture state. This layer and its evolution influence probe reflection. Therefore it is necessary to include the mixture optical properties into epsilon profile used in the Helmholtz equation
- Scales of phase grains is much smaller than the probe wavelength, therefore mixture can be described by its averaged dielectric function

$$\epsilon_{near\ sol}^{mix} = \epsilon^{sol} \left(1 + 3f \frac{\epsilon^{liq} - \epsilon^{sol}}{\epsilon^{liq} + 2\epsilon^{sol}} \right), \quad \epsilon_{near\ liq}^{mix} = \epsilon^{liq} \left(1 + 3(1-f) \frac{\epsilon^{sol} - \epsilon^{liq}}{\epsilon^{sol} + 2\epsilon^{liq}} \right)$$

$$\epsilon^{mix} = \epsilon_{near\ sol}^{mix} (1 - f^4) + \epsilon_{near\ liq}^{mix} f^4$$

- where expressions for epsilon^{mix} at small concentrations $f \ll 1$ or $1-f \ll 1$ are taken from Landau and Lifshitz “Electrodynamics of continuous media”
- For solid-liquid case relative difference between epsilon^{sol} and epsilon^{liq} is rather small. In this case we can use another expression from the same book valid at arbitrary concentration

$$\epsilon^{mix} = [f (\epsilon^{liq})^{1/3} + (1-f) (\epsilon^{sol})^{1/3}]^3$$

- Comparison of these two expressions shows that they give similar results

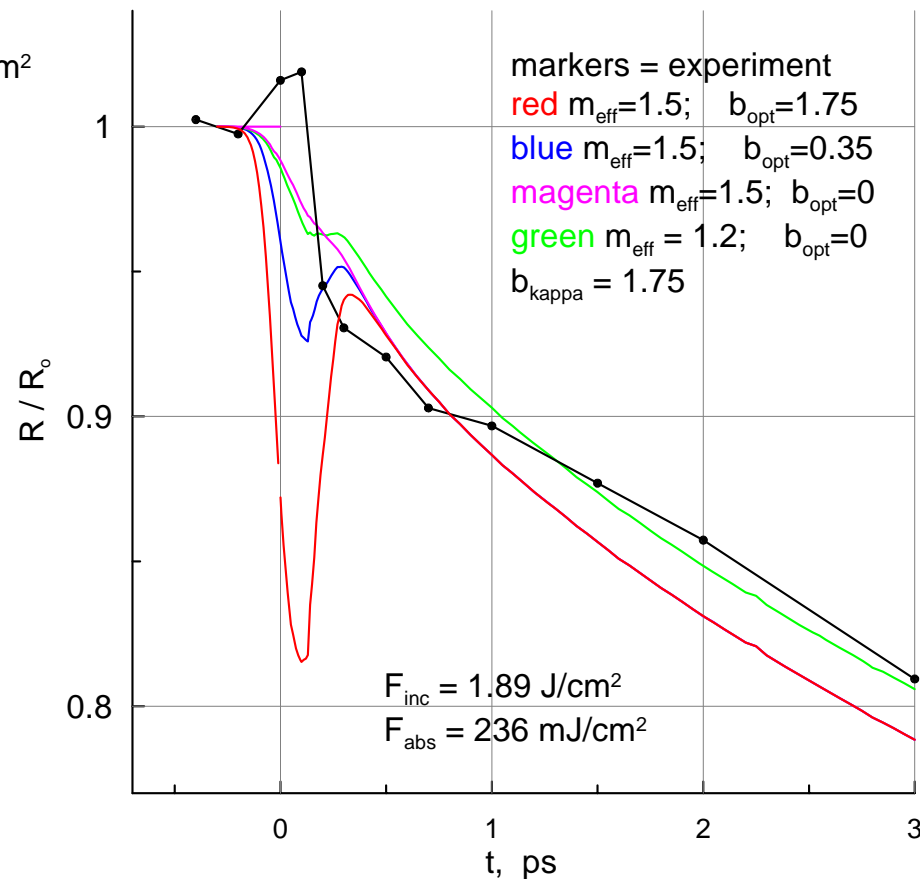
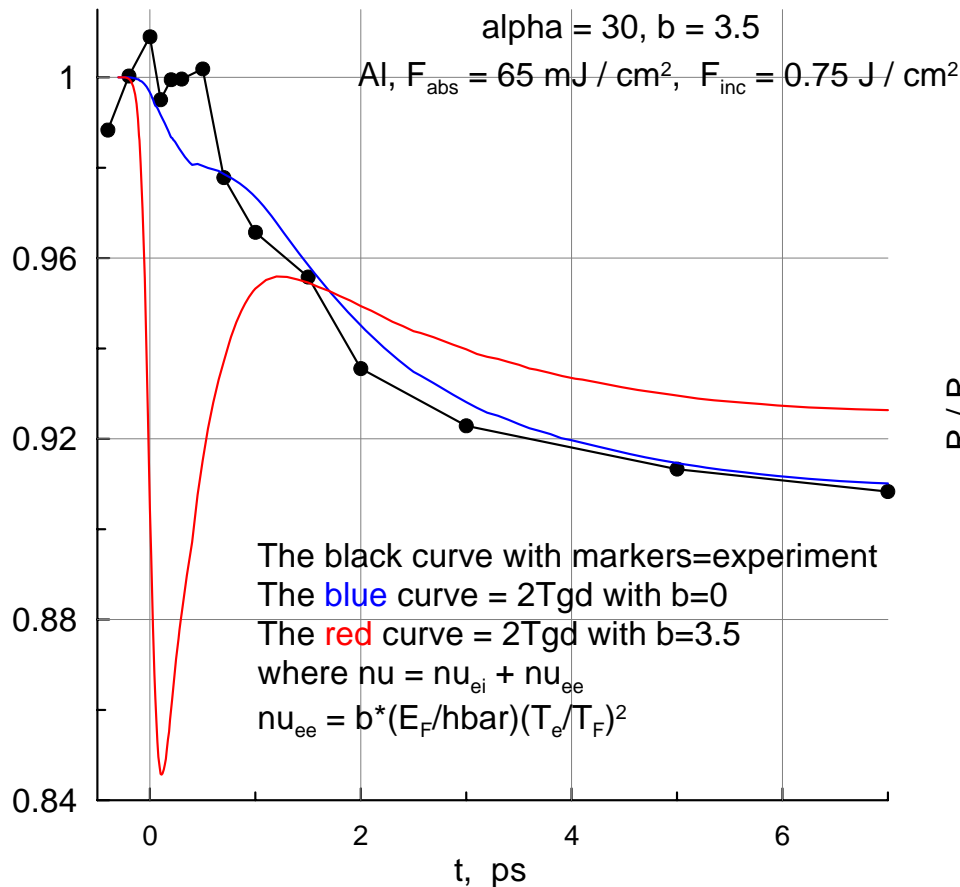
Probing of optical Properties of 2T Al (2T:

Te=high:17kK, 43kK)

$$\nu_{ee}^{opt} = b_{opt} (E_F / \hbar)(T_e / T_F)^2$$

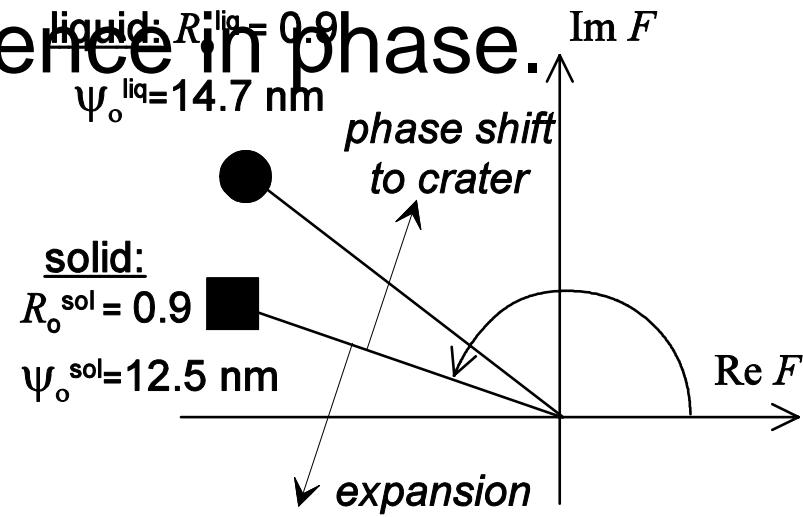
- ν_{ee} absorption is included into dielectric function
- ν_{ee} –if measured- should give **powerful diagnostic tool**: it left wing follows $T_e(t)$, while the right one gives history of melting since umklapp does not operate in melt

R / R₀: Reflectivity of prob fsLP normalized to Reflectivity before Pump

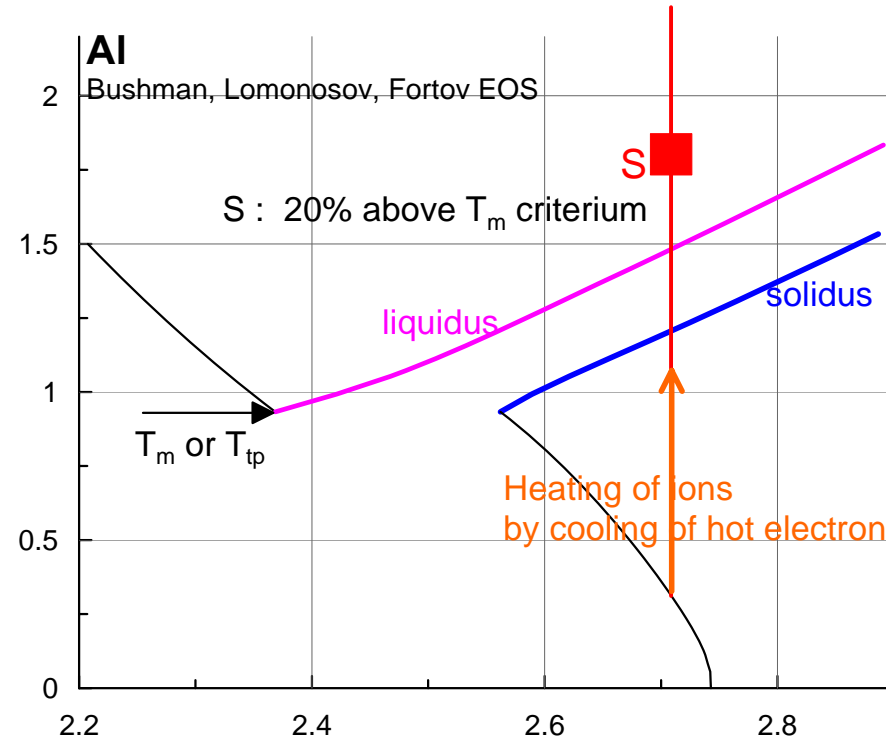
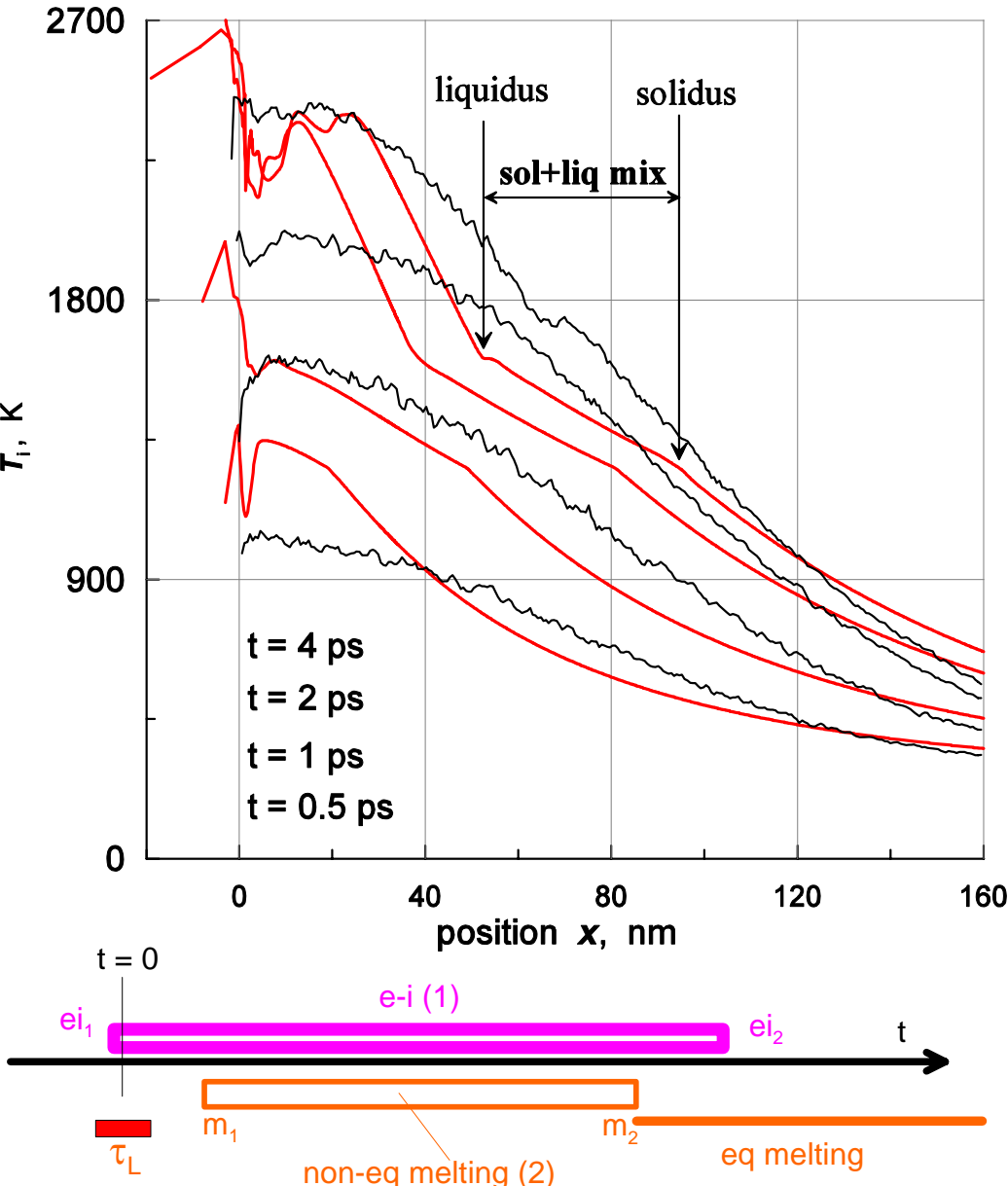


Probing of volume (supersonic) melting by phase measur-nts

- Above model and results for time history of reflection coefficient $R(t)$ have been presented
- Reflection may be measured by different technique but the pump-probe interferometry (PPI) has also advantage to measure phase $\Psi(t)$ of reflected probe wave. For Al difference in solid/melt R is small. Fortunately there is not large but measurable difference in phase.
- This opens possibility to follow phase $\Psi(t)$ (solid to liquid) evolution with PPI



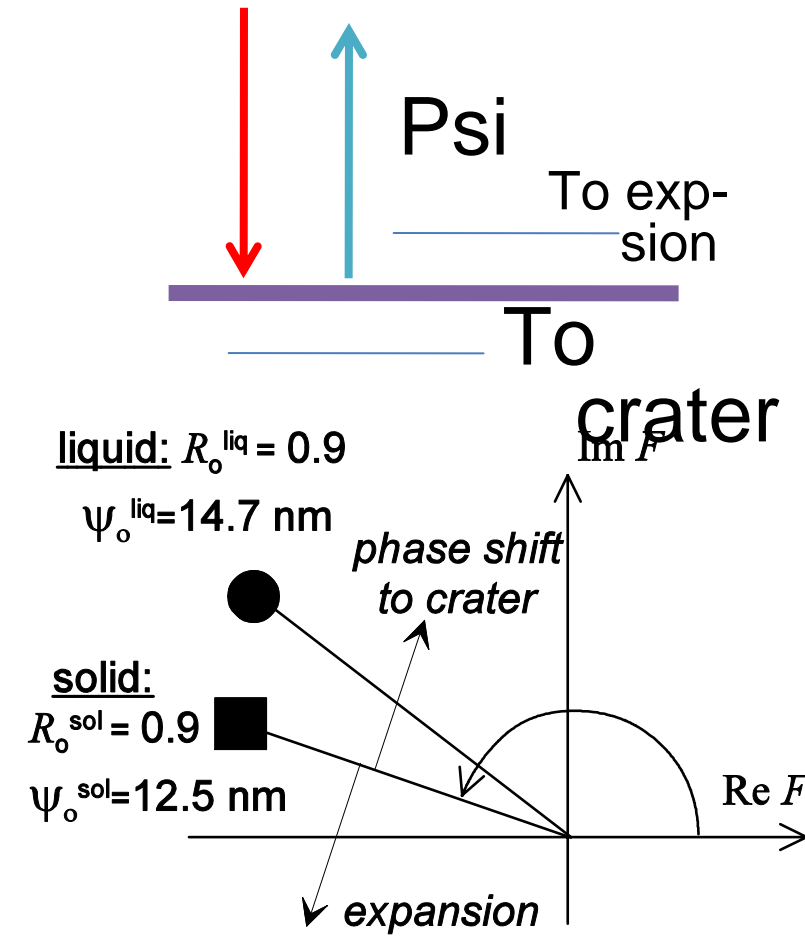
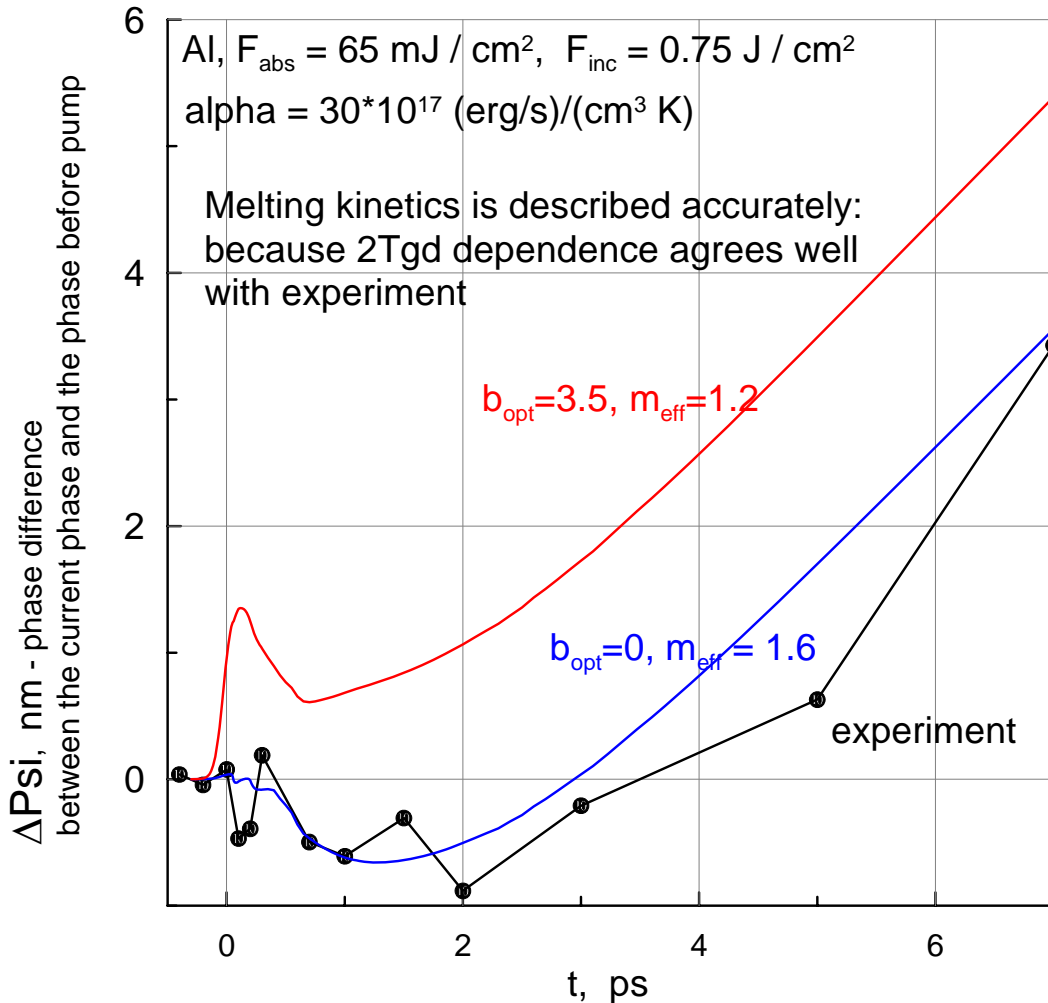
Heating of ion subsystem and changes in phase composition: solid \rightarrow melt



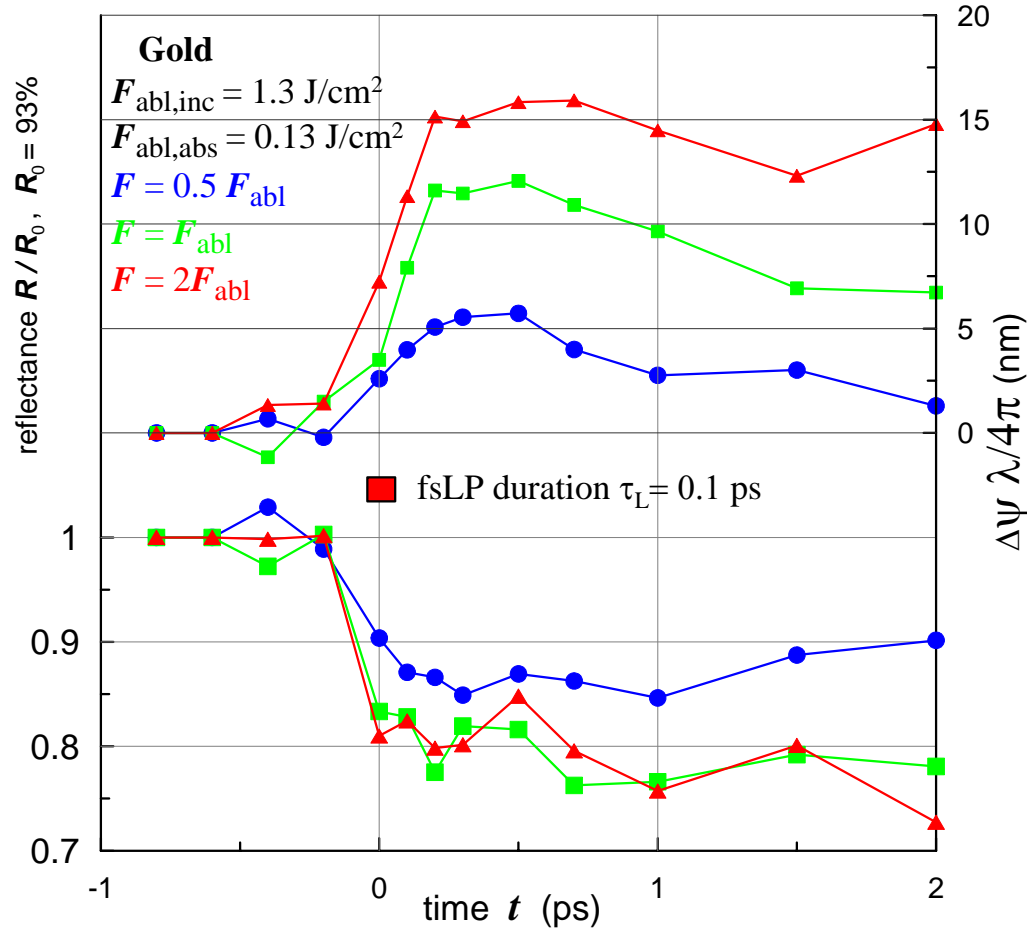
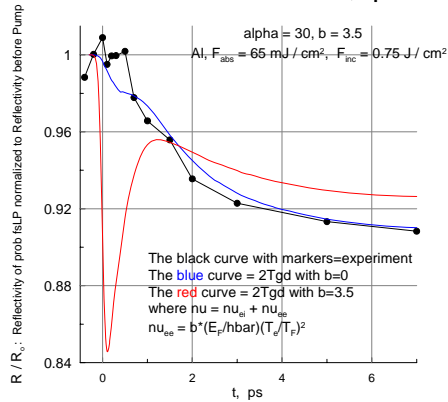
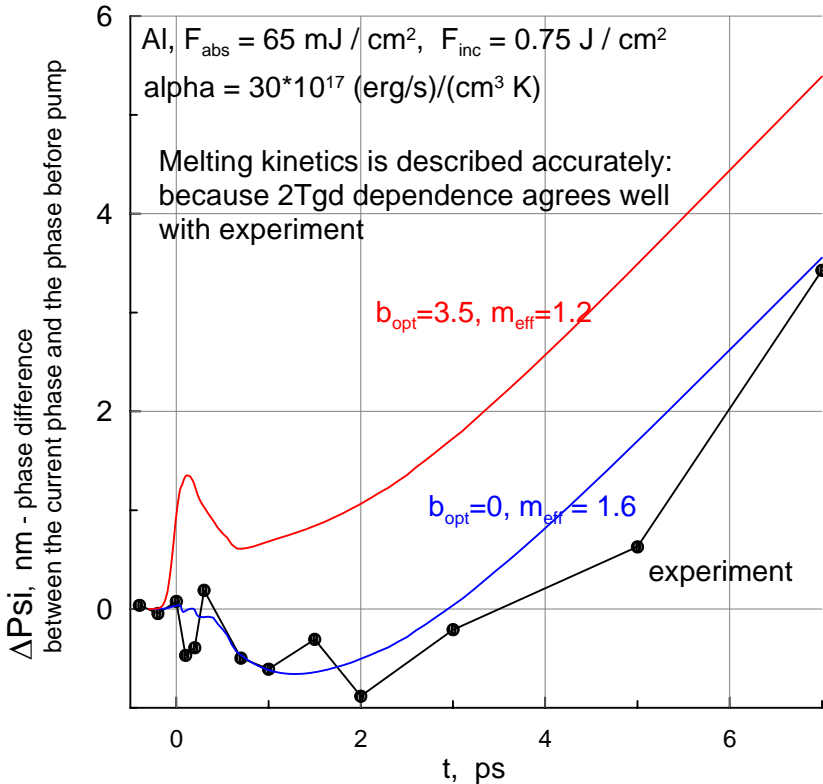
- T_e rises fast, T_i much slower
- Delay in melting due to thermal “inertia” of ions
- Overheated lattice, volume “supersonic” melting

Kinetics of Melting and the Phase Shift Evolution

- Phase shift relative to the phase of reflected light before the pump (from cold Al) is shown
- Agreement between simulated and experimental reflection means that our results capture melting from beginning



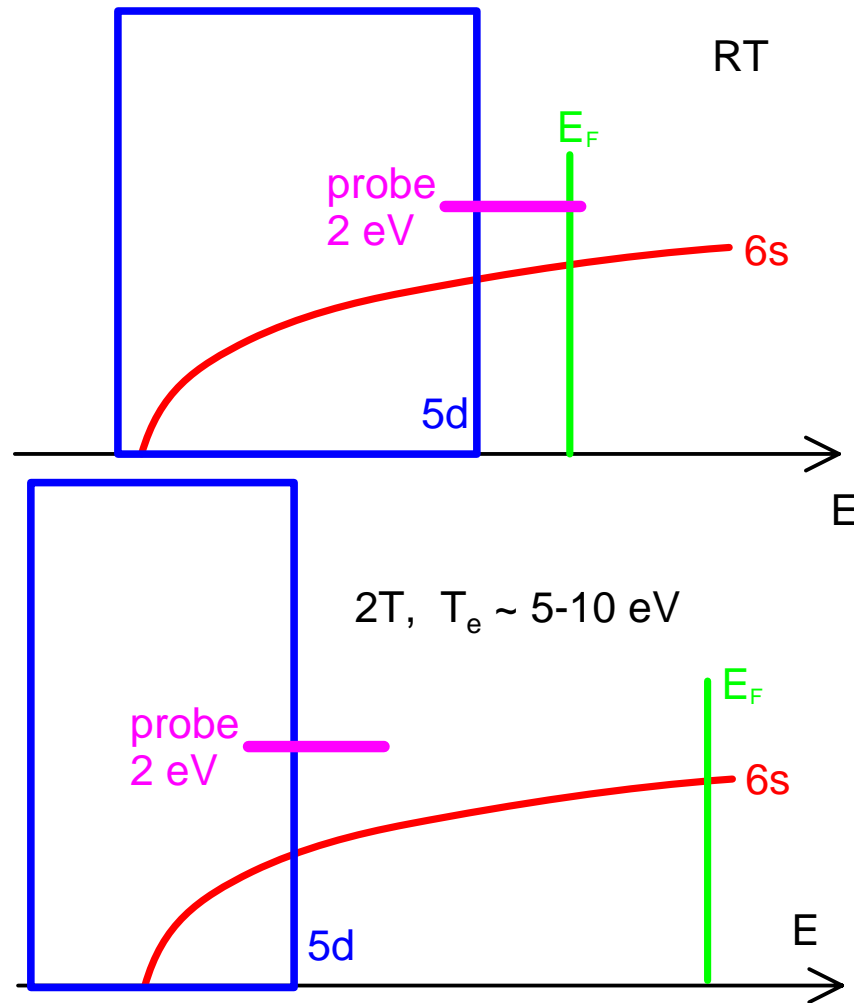
REFLECTANCE FOR ALUMINUM AND GOLD



Depletion of 5d zone and its shrinking and shift down

with T_e rise (lattice remains cold at $t \sim 1$ ps)

- Recoules et al., 2005 QM simulation



Excitation of 5d electrons into 6s+6p zone

- Definition of chemical potential
- Definition of number of excited electrons

$$z = z_s + z_d = \frac{\sqrt{2}}{\pi^2 n} \left(\frac{\sqrt{mkT}}{\hbar} \right)^3 \int_0^\infty \frac{\sqrt{x} dx}{\exp\left(x - \frac{\mu}{kT}\right) + 1} + gkT \ln \frac{1 + \exp\left(\frac{\mu - \varepsilon_1}{kT}\right)}{1 + \exp\left(\frac{\mu - \varepsilon_2}{kT}\right)}$$

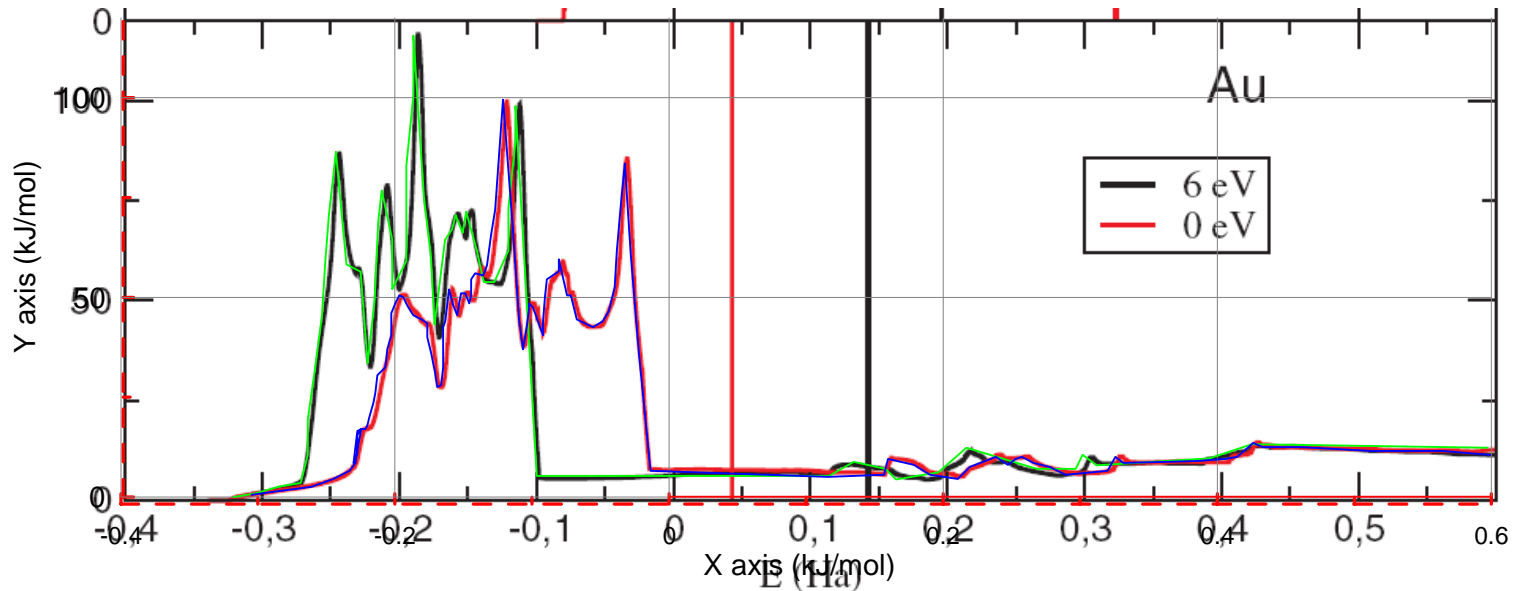
n – concentration of atoms, g – 5d DOS

The first term gives the number of electrons in 6s+6p zone per one atom.

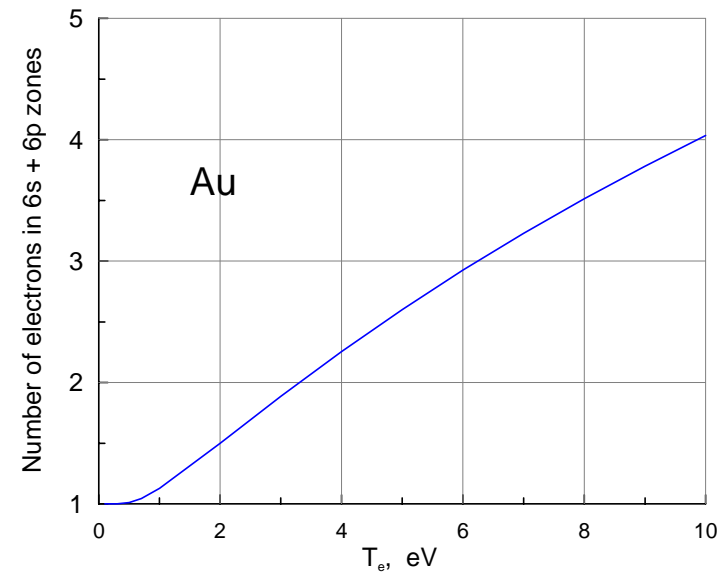
While the second is the number of electrons in 5d zone per one atom.

Excitation of 5d electrons into 6s+6p zone

- Shrinking and shifting of 5d zone due to changes in PSP as T_e increases. Similar to Recoules et al., PRL 2006.



- Growth of number of excited electrons. Linear approximation of shrinking and shifting of 5d zone



Band structure and plasma frequency is lost in very frequent e-e collisions?

- No umklapp as Brillouin cell of Au is smaller than Fermi sphere (opp.to Al)

- $Z = N_{e6s} \sim (2-4)$ for $T_e \sim (5-10)$ eV and weakly reacts (only $\sim 10\%$ in Z) on changes in band structure which seems large at the first glance

$$1.2 = 21 \frac{(\nu / \omega)}{1 + (\nu / \omega)^2} + 1 \quad 10 = 21Z \frac{(\nu / \omega)}{1 + (\nu / \omega)^2} + \Delta_i$$

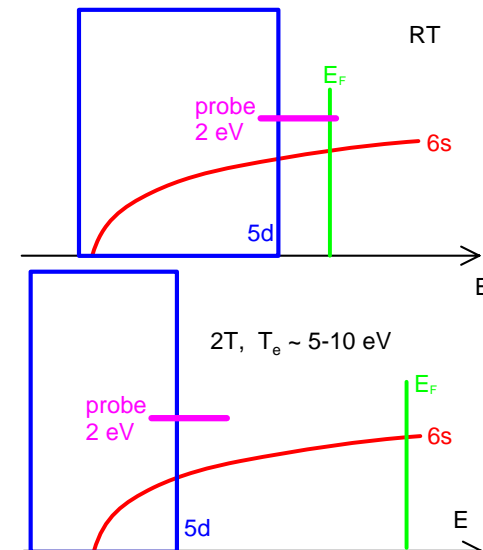
$$Z \sim 3$$

$$-9 = 1 - 21 + 11, \quad -14.5 = 1 - \frac{21Z}{1 + (\nu / \omega)^2} + \Delta_r$$

$$(\nu / \omega) \sim 2 - 3$$

Probe : $\omega = 3 \cdot 10^{15}$ (2eV), $\nu_0 = 0.01\omega$, $21 = (\omega_{pl} / \omega)^2$ at $Z_0 = 1, m_{eff} = 1$

- e-i seems weak as T_i is low and lattice symmetry unchanged
- Therefore e-e should dominate



Conclusion

- It is shown that in 2T Al n_{ee} addition in absorption is less than usually supposed
- Differences in optical properties of solid and liquid phase in metals are small. Therefore measurements of melting by interferometric pump-probe technique is not easy. These differences are much larger in the semiconductor case when liquid phase is metallic. In the presented work kinetics of melting has been followed by simulation and new experiments. It is shown that simulation describes situation
- Large difference between optical response of Al and Au to fsLP has been found
- New mechanism of nanorelief formation has been proposed. Scale of relief is of order of thermal penetration depth

Thank you for your kind
attention